The Role of Sphingolipids in Obinutuzumab-induced Direct Cell Death Mechanism

Sun Hyung Kwon

Department of Medical Science

The Graduate School, Yonsei University

The Role of Sphingolipids in Obinutuzumab-induced Direct Cell Death Mechanism

Sun Hyung Kwon

Department of Medical Science

The Graduate School, Yonsei University

The Role of Sphingolipids in Obinutuzumab-induced Direct Cell Death Mechanism

Directed by Professor Joo Young Kim

The Master's Thesis
submitted to the Department of,
The Graduate School of Yonsei University
in partial fulfillment of the requirements for the degree of
Master of Medical Science

Sun Hyung Kwon

December 2021

This certifies that The Master's Thesis of Sun Hyung Kwon is approved.

Thesis Supervisor: Joo Young Kim

Thesis Committee Member #1: Soo Han Bae

Thesis Committee Member #2: Wan Namkung

The Graduate School

Yonsei University

December 2021

ACKNOWLEDGEMENTS

First of all, I would like to thank Professor Joo Young Kim for giving me a chance to study in graduate school and helping me conduct experiments in the laboratory. Thanks to professor, I am glad to know how to plan the experiment and how to study. At first. I learned a lot from professor about how to go through the hard process, even if it's not necessarily related to the experiment. I am honored to enter the pharmacology class and run so far. Also, I am grateful to Professor Soo Han Bae and Professor Wan Namkung, who have advised me since the presentation of the research plan so that I can graduate even if my data was lacking a lot. Thanks to consideration and advice, my data was able to be completed a little more.

I would like to express my gratitude to Dr. Dong-hyuk Lee for giving and helping me experimentally despite his busy schedule in the lab room. Also, when I first came to the laboratory, I would like to thank Cho-eun kang for taking charge of various chores and teaching me various basic things and experiments during my experiment. Also, I would like to say thank you to Jung-yeol, who was able to talk the most in the lab room and helped a lot experimentally and externally. Also, I would like to express my gratitude to Do-hyun, Tae-young, and A-yeon and Ye-rim, who came into the laboratory and helped me a lot while working together since the beginning of this year.

Lastly, I would like to express my respection and gratitude to my father, who trusted me and actively supported me to go to graduate school and study, my mother, who always worried about me, and my brother who silently cooked me delicious food when I went home. I will try harder to repay all of you. Thanks.

TABLE OF CONTENTS

LIST OF FIGURES

ABSTRACT

The Role of Sphingolipids in Obinutuzumab-induced Direct Cell Death Mechanism

Sun Hyung kwon

Department of Medical Science

The Graduate School, Yonsei University

(Directed by Professor Joo Young Kim)

Obinutuzumab (OBI) is a third-generation therapeutic agent for CD20-targeted lymphoma with enhanced antibody-dependent cytotoxicity. The point is that OBI directly induces direct cell death (DCD) by simply binding to an antigen. This direct cell death is thought to be induced by the release of enzymes such as cathepsin B into the cytoplasm by lysosomal membrane permeabilization (LMP). However, the mechanism of LMP after OBI binding is not known.

In this study, we confirmed that OBI is endocytosis into lysosome through measuring the fluorescence change of pHAb labeled-OBI according to pH change. Also, we observed that filipin, known as an endocytosis blocker, reduces the OBI

induced DCD. Previously, we confirmed that the internalization of OBI blocks the TRPML2 channel and observed that it was related to the level of sphingomyelin (SM), a sphingolipid constituting the cell surface. When SM in the plasma membrane was degraded via bacterial sphingomyelinase (SMase), not only the inhibition of TRPML2 channel activity by OBI disappeared, but OBI-induced DCD was reduced. To demonstrate the critical role of SM endocytosis and degradation in the lysosome in OBI-induced DCD, bi-functional fusion antibodies were created by combining OBI with an enzyme that specifically degrades SM in acidic pH. It was observed that antibodies fused with acid sphingomyelinase (ASMase) showed enhanced DCD and antibody-dependent cellular cytotoxicity at low concentrations.

Taken together, we suggest that caveolae-dependent endocytosis of SM in plasma membrane along with OBI is important in DCD induced by OBI. Enhanced DCD by low concentrations of ASMase fusion antibody supports that subsequent SM degradation by ASMase in lysosome is essential for DCD.

Keywords: Obinutuzumab, CD20, sphingomyelin, sphingosine, acid sphingomyelinase, acid ceramidase, Lysosome membrane Permeabilization

The Role of Sphingolipids in Obinutuzumab-induced Direct Cell Death Mechanism

Sun Hyung Kwon

Department of Medical Science

The Graduate School, Yonsei University

(Directed by Professor Joo Young Kim)

I. INTRODUCTION

Lymphoma is the most common lymphoid malignancy including non-Hodgkin's lymphoma and Hodgkin's lymphoma. Non-Hodgkin's lymphoma, the majority (80-85%) of lymphomas, is considered more aggressive and unpredictable than Hodgkin's lymphoma[1-2]. Most B cell–derived lymphoma express a high level of CD20[2]. This CD20 surface antigen is expressed in a wide range starting from pre-B lymphocyte to germinal center mature B-cell[3-4]. However, the role of CD20 is still unclear[4-5]. The anti-CD20 monoclonal antibody (mAb) has been developed and used with chemotherapeutic agents[2]. For example, rituximab (RTX), developed for the treatment of non-Hodgkin lymphoma at the end of the 20th century, completely changed the treatment of lymphoma[2,6]. Also, since the anti-CD20 antibody has the

advantage of effectively depleting B cells, it has recently been attractive as a treatment for autoimmune diseases involving B cells[7].

Anti-CD20 mAbs are divided into two types, each of which shares features of killing effect and mechanism. Anti-CD20 mAbs have a variety of malignant B cell killing abilities such as antibody-dependent cell cytotoxicity (ADCC), complement-dependent cytotoxicity (CDC), and antibody-dependent cell phagocytosis (ADCP)[8]. Type I anti-CD20 mAbs including RTX, show strong CDC which is caused by the recruitment of complement components. On the other side, type II anti-CD20 mAbs are characterized by potent DCD and ADCC[9]. ADCC occurs by a process that effector cells such as natural killer (NK) cells recognize the FC region of antibody which is binding to surface antigen and release the cytotoxic molecules to kill the infected cell or cancer cell[10]. However, the most characteristic and ambiguous part is the DCD mechanism.

Obinutuzumab (OBI) is a glycoengineered humanized type II anti-CD20 mAb. This glycoengineering results in the defucosylated IgG Fc region, which has enhanced affinity to the FcγIII of NK cell[11]. As mentioned previously, OBI induces potent direct binding cell death ability as a type II antibody[11]. The DCD induced by OBI is the result of a serial process. OBI-induced lysosome swelling leads to lysosome rupture called lysosomal membrane permeabilization (LMP). Finally, lysosomal degradative enzymes such as cathepsin B are released in the cytosol and induce reactive oxygen species (ROS) occurrence which is directly connected to non-apoptotic cell death[13-14]. It seems that LMP carries out a critical role in OBI-induced DCD.

A lysosome is an intracellular vesicle carrying a lot of lysosomal enzymes and ion channels. Lysosome has various hydrolytic enzymes involved with cellular molecules such as lipid, protein, carbohydrates, which are associated with cell signaling by several degradation pathways[15,16]. Also, these enzymes are usually working in lysosomal acidic pH maintained by V-ATPase on the lysosomal membrane.

Especially, autophagy is the best-known lysosome-mediated degradation pathway to maintain cellular homeostasis[17]. In the beginning, phagophore encloses protein aggregates, the intracellular damaged subcellular organelle. Autophagosome completely enclosed phagophore, merge with lysosome during maturation. Then, lysosomal enzymes promote breaking down the contents from the autophagosome. Through this pathway, a cell reuses the byproduct of degradation[18].

Normally, glycoproteins such as Lamp-1 or Lamp-2 are expressed at high levels for keeping the lysosome membrane intact from lysosomal low pH and enzymes by forming a glycocalyx layer inside of the lysosome membrane[19]. However, once lysosomotropic factors such as sphingosine, TNF-α, and siramesine destabilize the membrane, then the lysosomal membrane gets ruptured and lysosomal enzymes are released[20-21]. Although somewhat ambiguous, it is known that lmp induces apoptosis.[21]. The lysosomotropic agents, which are accumulated to the lysosomal membrane and destabilize the membrane balance, intend to be more toxic in various cancers[21,23-24].

SM, which generates sphingosine, a lysosomotropic factor, is involved with DCD induced by type II anti-CD20 antibody[25]. DCD induced by type II antibodies depend on the level of SM in the plasma membrane[26]. The sphingolipid such as sphingosine, ceramide and SM is a type of phospholipid that has a sphingoid backbone containing sphingosine backbone and various carbon chain structure[27]. Each member of sphingolipid carries out an important role as a cellular signaling mediator because of its bioactivities.

SM enriched in the plasma membrane is a fully saturated fatty acid. Cholesterol tends to have a stable interaction with saturated fatty acids, and thus tends to interact with SM over other phospholipids, which affect the membrane property and recruitment of transmembrane protein in the plasma membrane[28-29]. Also, SM which forms lipid microdomain including caveolin-1 is involved in caveolar endocytosis[30].

The level of each sphingolipid member is regulated by a variety of enzymes that are involved in sphingolipid metabolism and sphingolipid biogenesis[31-32]. There are lysosomal enzymes that degrade each sphingolipid specifically at low pH. Acidic sphingomyelinase (ASMase) is a lysosomal enzyme that breaks down SM to ceramide[32]. ASMase is known to consist of a saposin domain and a catalytic domain. Saposin domain is interacting with membrane and makes substrates accessible to the catalytic domain, which is necessary to the activity of ASMase[33]. But ASMase undergoes various post-translational modifications. After successful translation, the disulfide bridge in ASMase is formed by disulfide bond isomerase in the ER lumen and undergoes C-terminal modification by enzymes such as β-glucosidase and cathepsin D in the lyososome[34].

In this study, we found that filipin (an inhibitor of caveolae-dependent endocytosis) not only decreased endocytosis of OBI into acidic organelles, but also decreased OBI-induced DCD. In addition, the reduced SM in the plasma membrane by bacterial SMase not only reversed OBI-induced TRPML2 channel inhibition, but also reduced OBI-induced DCD. To prove the importance of SM degradation in acidic organelles, 4 forms of bi-functional OBI fused with enzymes decomposing SM were generated to accelerate SM degradation after endocytosis. ASMase fusion OBI, not acidic ceramidase (ACDase) fusion OBI, showed increased DCD at low concentrations. Based on this finding, we concluded that delivery and decomposing of SM into acidic organelles along with OBI endocytosis is critical for OBI-induced DCD.

II. MATERIALS AND METHODS

1. HEK 293T transfection for Lentivirus production

HEK 293 T cells were maintained in DMEM media (# LM 001-01, Welgene) supplemented with 10 % FBS (# 16000-044, Gibco) and 1 % penicillin/streptomycin (# LS202-02, Welgene) at 37 °C in 5 % CO_2. Seeding 0.8 x 10^6 HEK 293T cells each well on a 6 well plate. After 24 hours, PEI (# 23966-1, Polysciences, Warrington, US) (1 mg / ml) and lentiviral plasmid vectors (pMD2g : psPAX2 : lentiviral vector = 0.25 μg : 0.75 μg : 1 μg) are mixed according to the protocol recommended from Addgene. After 16 hours, DMEM media should be changed up to 6 ml and incubated for 48 hours.

2. Generation of mAb-producing CHO-K1 cells

CHO-K1 cells were maintained with RPMI full media supplemented with 10 % FBS and 1 % penicillin/streptomycin at 37°C in 5 % CO_2. Seeding 0.3 ~ 0.5 x 10^5 CHO-K1 cells each well on a 12 well plate. After overnight, cells were incubated with polybrene (# 2920949, sigma, St. louis, Missouri, USA) with 10 μg / ml in 600 μl RPMI full media for 5 hours. After incubation, lentivirus including DNA of antibody's heavy chain and light chain were added to cells in a PLVX-CIBleo-light chain lentivirus: PLVX-CIP-heavy chain lentivirus = 300 μl : 700 μl ratio. After 16 hours, the media containing lentivirus is replaced with fresh media. CHO-K1 Cells were selected with antibiotics puromycin (# ant-pr-1 Invivogen, San Diego, California, USA) with 8 μg/ml and blasticidin S (# SMB001-100MGS, Biomax) with 16 μg/ml.

3. Purification of mAb

CHO-K1 expressing antibody cells grown to 80~90% confluence on 100 cm petri dish in RPMI full media were washed twice with PBS (# PR4007-100-00, Biosesang). CD CHO media (# 10743029, Gibco, Waltham, Massachusetts, USA) supplemented with L-glutamine with 8 mM final concentration and 1mM sodium butyrate (# LS033-01, Welgene) was added to cells. CHO cells with CHO media were incubated for 3 weeks at 30°C in 5% CO_2. CHO media was incubated via protein A agarose (# 20333, Thermoscientific, Waltham, Massachusetts, USA) to purify antibodies for overnight. Antibodies were eluted from the resin via 0.1 M citric acid buffer. Buffer change was conducted by Slide-A-Lyzer™ Dialysis cassettes (#66330, Thermoscientific, Waltham, Massachusetts, USA) and antibody concentration was carried out via Amicon® Ultra-4 Centrifugal Filter Unit (# UFC810008, Merck, Darmstadt, Germany). 7 μM purified antibody was loaded to PAGE gel for SDS-PAGE and stained via coomassie brilliant blue R-250 (# CR1031-025-00, Biosesang).

4. Bi-functional fusion antibody cloning

Bi-functional fusion antibodies were cloned by fusion of the c-terminal of the OBI heavy chain with two enzymes, ASMase and ACDase. For appropriate enzyme activity of ASMase, three structures were designed. The ASMase and ACDase clones were purchased from Sino Biological (# HG11087-M, Beijing, China) and Korea Human Gene Bank (# BKU002034) respectively. The detail sequences of used OBI are following:

OBI light chain amino acid sequence

MDMRVPAQLLGLLLLWFPGARCDIVMTQTPLSLPVTPGEPASISCRSSKSLLH
SNGITYLYWYLQKPGQSPQLLIYQMSNLVSGVPDRFSGSGSGTDFTLKISRVE
AEDVGVYYCAQNLELPYTFGGGTKVEIKRTVAAPSVFIFPPSDEQLKSGTASV
VCLLNNFYPREAKVQWKVDNALQSGNSQESVTEQDSKDSTYSLSSTLTLSK
ADYEKHKVYACEVTHQGLSSPVTKSFNRGEC

OBI heavy chain amino acid sequence

MDWTWRILFLVAAATGAHSQVQLVQSGAEVKKPGSSVKVSCKASGYAFSYS
WMNWVRQAPGQGLEWMGRIFPGDGDTDYNGKFKGRVTITADKSTSTAYME
LSSLRSEDTAVYYCARNVFDGYWLVYWGQGTLVTVSSASTKGPSVFPLAPSS
KSTSGGTAALGCLVKDYFPEPVTVSWNSGALTSGVHTFPAVLQSSGLYSLSSV
VTVPSSSLGTQTYICNVNHKPSNTKVDKKVEPKSCDKTHTCPPCPAPELLGGP
SVFLFPPKPKDTLMISRTPEVTCVVVDVSHEDPEVKFNWYVDGVEVHNAKT
KPREEQYNSTYRVVSVLTVLHQDWLNGKEYKCKVSNKALPAPIEKTISKAKG
QPREPQVYTLPPSRDELTKNQVSLTCLVKGFYPSDIAVEWESNGQPENNYKTT
PPVLDSDGSFFLYSKLTVDKSRWQQGNVFSCSVMHEALHNHYTQKSLSLSPG
K

About OBI fusion antibody with ASMase (Obi-ASMase wild type), C-terminus of OBI heavy chain is fused with N-terminus of ASMase (RefSeq NM_000543.3, NP_000534.3, amino acid residues 47-631). Two-part of this protein were linked via two peptides -AS- (Nhe I restriction site). In the case of Obi-GFLG-ASMase and Obi-DEVD-ASMase, the C-terminus of the OBI heavy chain is fused with the N-terminus of ASMase (amino acid residues 85 to 630). Also, -AS DEVD- and –AS GFLG- linked the two domains of the fusion protein. In addition, Obi-ACDase (RefSeq

NM_177924.5, NP_808592.2, amino acid residues 22-395) wild type was created in the same manner as Obi -ASMase wild type.

5. Antibody conjugation with pH sensor dye, pHAb

Antibody was conjugated with pHAb amine-reactive dye (# G9845, Promega, Madison, Wisconsin, USA) according to the manual. The purification process was conducted according to Dylight™ 550 Microscale antibody labeling kit (# 84531, Thermoscientific, Waltham, Massachusetts, USA) via spin column and purification resin.

6. Antibody internalization assay

9 x 10^5 Raji cells were incubated in PBS containing antibody with a final concentration of 10 μg / ml for 1 hour at 4 ℃. After incubation, cells were washed to remove unbound antibodies and resuspended with PBS. For inhibition of internalization, Raji cells were pretreated with filipin or dynasore. Fluorescence was measured by FACSverse (BD bioscience). The fluorescence intensity change ratio was calculated as the change of fluorescence intensity (ΔF) which was normalized with the first fluorescence intensity (F_0) every indicated time.

7. Antibody binding assay

1.5 x 10^5 Ramos cells were prepared in 25 μl PBS. Antibody with 1 μg/ml, 3 μg/ml, 10 μg/ml in 25 μl PBS was added to Ramos cells for 1 hour at 4℃. After 1 hour, Ramos cells were washed with PBS and resuspended with 100 μl goat anti-human IgG Alexa

647 (3 μg/ml) (# 109-605-003, Jackson ImmunoResearch, West Gove, Pennsylvania, USA) for 30 min at 4 ℃. After incubation, Ramos cells were washed with PBS twice and resuspended with 200 μl PBS. Fluorescence was measured by FACSverse.

8. Measurement of complement-dependent cytotoxicity

For complement-dependent cell death, 2 x 10^5 Ramos cells were prepared in 50 μl RPMI full media and incubated with a final concentration of 0.125 μg/ml calcein-am (# 425201, Biolegend, San Diego, California, USA) for 30 min at 37 ℃. After washing the Ramos cells, cells were incubated with antibodies (0.7 nM, 2.1 nM, 7 nM, 21 nM) for 10 min at 37℃ in 5 % CO_2. 6 μl of complement rabbit MA (# CL3221, Cedarlane, Burlington, Canada) was added to cells and incubated for 2 hours. Calcein-AM-stained cells were considered live cells and the death rate (%) (100 % - % of live cells) was calculated by FACSverse (BD bioscience).

9. Purification of PBMC cells and measurement of antibody-dependent cellular cytotoxicity

PBMC from healthy donors who voluntarily participated in our study according to IRB procedure approved by the committee of Yonsei IRB board. 5 ml blood was briefly mixed with 5 ml PBS then the mixture was added to 3 ml Histopaque-1077 (# 10771, Sigma, St. louis, Missouri, USA) which had been laid down in 15 ml conical tube. For antibody-dependent cell death, 2 x 10^5 Ramos cells were prepared in 50 μl RPMI full media and incubated with a final concentration of 0.125 μg/ml Calcein-AM (# 425201, Biolegend, San Diego, California, USA) for 30 min at 37℃ in 5 % CO_2. After washing the Ramos cells, cells were incubated with PBMC cells with 1: 5 ratio. Antibodies (0.7

nM, 2.1 nM, 7 nM, 21 nM) were added and incubated for 4 hours at 37 ℃. Calcein-AM-stained cells were considered live cells and the death rate (%) (100 % - % of live cells) was calculated by FACSverse (BD bioscience).

10 Measurement of antibody-induced direct cell death

2 x 10^5 Raji cells are incubated with 0.7 nM, 2.1 nM, 7 nM, and 21 nM antibody in 100 µl reaction volume of RPMI full media at 37℃ in 5 % CO_2 for 6 hours. After incubation, cells were stained with 100 µl of 0.25 µg/ml calcein-AM at 37℃ in 5 % CO_2 for 30 min. Calcein-AM-stained cells were considered live cells and the death rate (%) (100 % - % of live cells) was calculated by FACSverse (BD bioscience).

11. Enzymatic assay for measurement of ASMase activity

1.32 mmol/L HMU-PC (# EH31028, Sigma, St. louis, Missouri, USA) was prepared in distilled water. 10 µl of 17 nM antibody, 10 µl of 0.1 M sodium acetate buffer (pH 5.2) containing 0.2% (w/v) synthetic sodium taurocholate (#102H5011, Sigma, St. louis, Missouri, USA), and 0.02% sodium azide were mixed on black 96-well plate, in advance. After HMU-PC was added to the mixture with 10 µl of 10 mM sphingomyelin (# S0756, Sigma, St. louis, Missouri, USA) or not, the mixture was incubated for 5 hours at 37℃. The stop solution containing 0.2 mol/L glycin-NaOH buffer (pH 10.7), containing 0.2% (w/v) sodium dodecyl sulphate and 0.2 % (w/v) Triton X-100 was added to the mixture after incubation. The fluorescence was measured by a microplate reader with 360 nm /460 nm.

12. Measurement TRPML2 activity by change of calcium-indicator fusion protein, GCaMP-TRPML2

The GCaMP-TRPML2 plasmid was transfected in Ramos cells. 48 hours after transfection, the change of GCaMP fluorescence was monitored using confocal microscopy (LSM710 Zeiss, Germany). The cells were continually perfused in 1.5 mM Ca^{2+} regular solution containing 150 mM NaCl, 5 mM KCl, 1 mM $MgCl_2$, 10 mM HEPES (pH 7.4 adjusted with NaOH), then cells were treated with indicated mAbs (10 μg/ml) for 5 min. The TRPML2 specific Ca^{2+} channel activity was measured by the treatment of ML-SA1 (20 μM), a TRPML channel-specific activator. The fluorescence intensity change of GCaMP-TRPML2 was calculated as the change of fluorescence intensity (ΔF) normalized by the first fluorescence intensity (F_0) in the specific cell region.

13. Statistical analysis

Data are presented as the means ± standard error of the mean. Statistical analysis was performed with student's t-test, followed by Tukey's multiple comparisons using the GraphPad Prism software package (version 5.0), as appropriate. $P<0.05$ was considered statistically significant.

III. RESULTS

1. Endocytosis of obinutuzumab into acidic organelles after CD20 binding

It is well-known that RTX is internalized by binding to CD20 on the plasma membrane. Internalization of RTX is conducted by FcγRIIb and considered a process of getting resistance to RTX-induced killing effect by lymphoma[35]. But, whether the OBI is internalized or not has been unclear. We conjugated the pH-sensing molecule, pHAb, to antibodies. Conjugated antibodies release fluorescence depending on the acidity around the antibody (Fig.1A). Successful conjugation of antibody was confirmed in SDS-PAGE gel by Ph-dependent fluorescence (Fig.1B). Antibody-dylight (Obi-dylight, Rit-dylight) showed fluorescence regardless of pH. Antibody internalization assay was performed during 10, 30, 60, 90, 120 min at 37℃ after the 10 μg/ml-antibodies treatment. OBI showed a faster and higher increase of fluorescence than RTX (Fig.1C). OBI showed noticeable fluorescence changes from 10 min and plateau from 60 min. RTX showed the similar trend, but the fluorescence change of RTX was much less than it of OBI. Considering that the binding affinity of OBI is only half of RTX, the internalization of OBI is likely to reach very acidic organelles, such as lysosomes. This result suggests that when OBI binds to CD20, OBI is endocytosis to the acidic organelles, endo/lysosome.

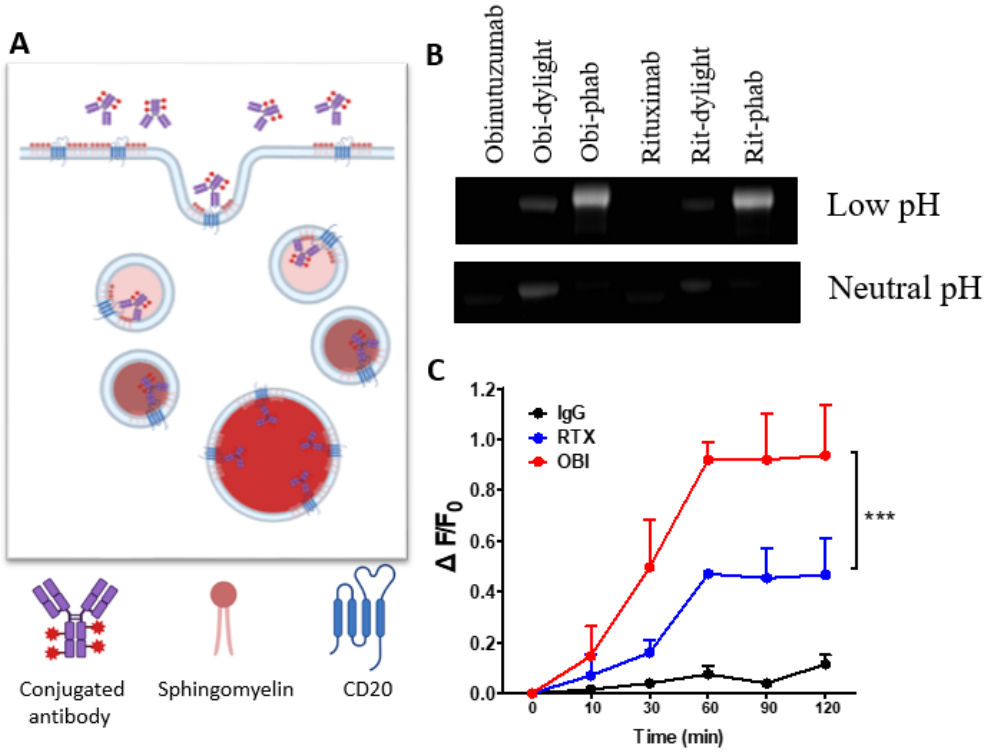

Figure 1. Obinutuzumab-pHAb endocytosis into the acidic organelle (A) Schematic image of endocytosis process of conjugated antibody (B) SDS-PAGE running of OBI-pHAb and Rituximab-pHAb (Rit-pHAb). The SDS-PAGE gel was incubated in pH 3.0 distilled water for 30 min or just distilled water. (C) The fluorescence intensity change ratio of pHAb-conjugated IgG, RTX, and OBI. Raji cells were incubated with 10 μg/ml of each anti-CD20 antibody for 1 hour at 4 ℃. After incubation, cells were washed with cold PBS buffer. Cells were incubated at 37 ℃ on a heat block for the indicated time. Then, fluorescence was measured by FACS every indicated time. OBI-pHAb released fluorescence greater than Rit-pHAb or IgG-pHAb. Data are presented as the mean±SEM. ***$p<0.001$ vs. control

2. Decreased obinutuzumab-induced DCD by blocking of obinutuzumab-endocytosis

OBI is known to cause lysosomal swelling in a short time (about 30 min to 1 hour), and eventually the lysosome bursts (after about 1 hour). The LMP seems a very important process for OBI-induced DCD. In Figure 1, we demonstrated that OBI internalizes rapidly into the acidic organelles. To determine whether the endocytosis is related to OBI-induced DCD, we carried out a DCD assay with two representative endocytosis inhibitors, filipin and dynasore. Filipin is known to prevent caveolae-mediated endocytosis by fixation of cholesterol, and dynasore is known to prevent clathrin-dependent endocytosis by blocking GTPase activity of dynamin[36-38]. To check which endocytosis pathway is related to OBI endocytosis, filipin and dynasore were pretreated in Raji cells and measured the fluorescence change of OBI-pHAb for 1 hour. Both treatments inhibited the fluorescence change of OBI-pHAb, but the filipin showed stronger inhibition (Fig. 2A). In addition, DCD caused by OBI was reduced with filipin, but DCD caused by OBI was not affected by dynasore (Fig. 2B). These data suggest that OBI reduces DCD because of reduced internalization by filipin. Accordingly, the caveolae-dependent endocytosis of OBI is the critical process of DCD by OBI.

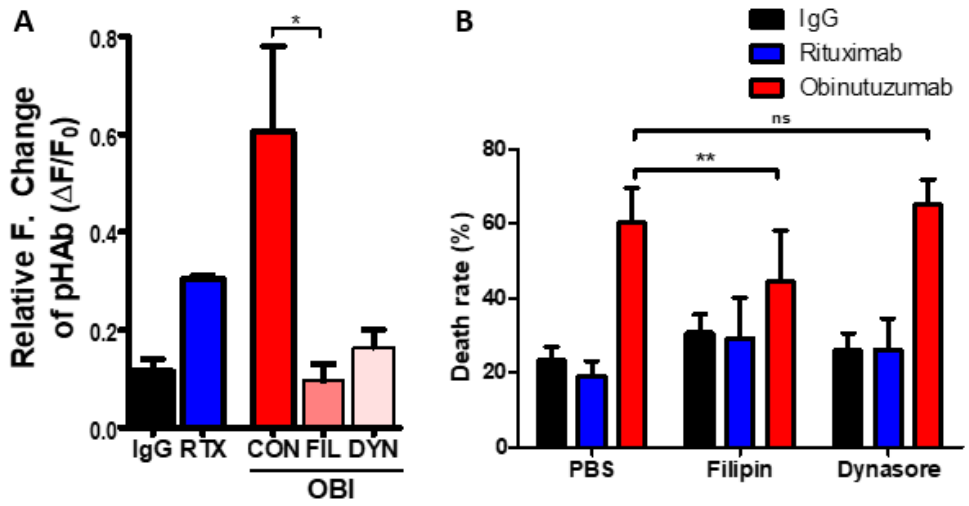

Figure 2. Inhibition of obinutuzumab-induced direct cell death by filipin, a caveolae-mediated endocytosis blocker. (A) Relative fluorescence change of antibody labeled with pHAb dye. Filipin and dynasore were pretreated for 30 min at 37 °C. Raji cells were incubated for 1 hour at a concentration of 10 μg/ml of conjugated antibody. (B) Direct cell death assay with filipin and dynasore. Raji cells were incubated at 10 μg/ml OBI for 6 hours. Filipin (80 μM) and dynasore (10 μM) were pretreated for 30 min at 37°C. Data are presented as the mean±SEM. *$p<0.05$, **$p<0.01$ vs. control.

3. Reduced obinutuzumab-induced DCD by sphingomyelin depletion in the plasma membrane

TRPML channels located in the endo/lysosome include TRPML1, TRPML2, and TRPML3[39]. The TRPML channel functions to release Ca^{2+} from the inside of the lysosome, and the normal function of the channel plays an important role in lysosomal traffickings such as fusion or fission between the lysosome and other organelles[40]. In previous research, we found OBI inhibit the Ca^{2+} channel activity of the TRPML2 channel in the lysosome. When cells were treated with OBI, ML-SA1 induced Ca^{2+} channel activity of TRPML2 was inhibited. Given that GPN, a non-specific lysosome Ca^{2+} ionophore-induced activity of TRPML2 was not affected, OBI specifically inhibits TRPML2 after endocytosis. Interestingly, the activity of TRPML channels is inhibited by SM[41]. The amount of SM in the plasma membrane is associated with type II anti-CD20 antibody-induced DCD. Based on these observations, we hypothesized that OBI-binding to CD20 would induce internalization of SM on the plasma membrane and inhibit the TRPML2 channel activity. To demonstrate this, the activity of TRPML2 was measured after SM in the plasma membrane was degraded by bacterial SMase which is active in neutral pH. In the case of heat-inactivated bacterial SMase, OBI inhibited the TRPML2 channel activity (Fig. 3A). We observed that the ability of OBI to inhibit TRPML2 channel activity was disappeared by treatment with 50 ng and more inhibited with 5000 ng bacterial SMase (Fig, 3B, 3C). Next, we observed whether the treatment of bacterial SMase affects DCD caused by OBI. We incubated Raji cells with 10 μg/ml antibody at 37 ℃ for 6 hours after pre-treatment of active bacterial SMase or heat- inactivated bacterial SMase for 30 min. We found that OBI-induced DCD was decreased by bacterial SMase, not by the inactive form of SMase (Fig. 3D). These data suggest that OBI-induced DCD is dependent on the internalized SM.

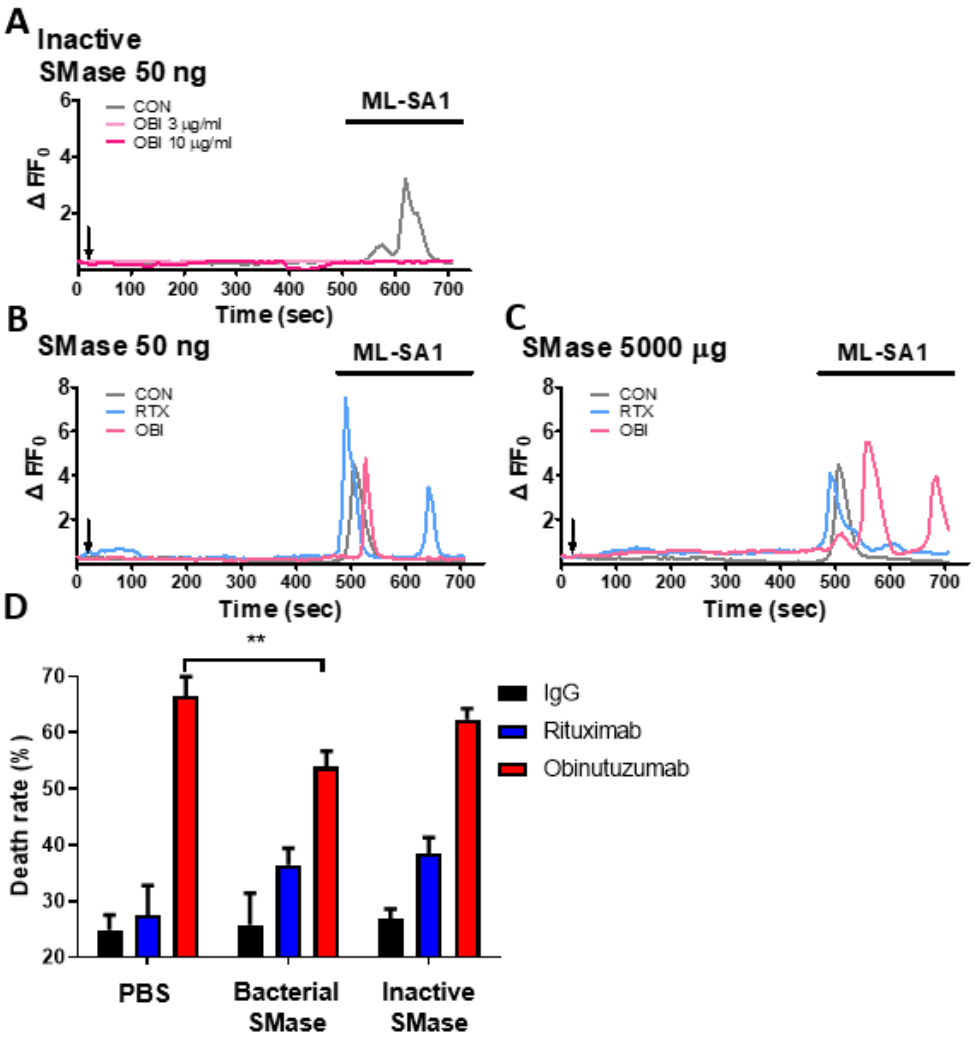

Figure 3. Abolished obinutuzumab-inhibited TRPML2 Ca^{2+} channel activity and decreased direct cell death by bacterial sphingomyelinase. Mean GCaMP-TRPML2 fluorescence traces of Ramos cells. ML-SA1 was used as a TRPML2 channel activator. Ramos cells were pretreated with 50 ng inactive bacterial SMase (A) 50 ng (B) and 5000 ng SMase (C) at 37℃. (D) OBI induced direct cell death assay. Raji cells are incubated with a bacterial SMase, inactive bacterial SMase at

37°C heat block for 30 min. After washing the cells, incubate the cells in 10 μg/ml antibody for 6 hours. Calcein-AM staining was performed for 30 min to measure fluorescence through FACS. Data are presented as the mean ± SEM. **$p<0.01$ vs. control.

4. Preserved affinity and enzyme activity in ASMase fusion obinutuzumab

We found that OBI would be internalized in the lysosome together with SM. It seems that the SM internalized to the lysosome by OBI is degraded into sphingosine, which induces destabilization of the lysosomal membrane. So, we designed a fusion antibody by attaching enzymes to the c-terminus of the OBI heavy chain for enhancing lysosomal sphingolipid metabolism after SM internalization. OBI-ASMase wild type (Obi-ASMase wt) was made through a fusion of N-terminal ASMase (amino acid residues 47-631 without signal sequence). Also, there is a report that N-terminal residue (47-84) and c-terminus (C631) deletion is required for ASMase's activity [33-34,42-43]. Because the N-terminal saposin domain of ASMase is required for membrane docking, which is essential for SM degradation[42], we are concerned the saposin domain would be affected by the IgG Fc region. So, by attaching a lysosomal degradable 4 peptide linker such as GFLG or DEVD to a modified enzyme (amino acid residues 85-630), OBI-GFLG-ASMase (Obi-GFLG-ASMase) and OBI-DEVD-ASMase (Obi-DEVD-ASMase) were designed to induce the release of ASMase from the lysosome (Fig. 4A). The designed antibodies were prepared by lentivirus infection to produce a CHO-K1 stable cell line, and the antibody was purified by incubation of CHO-K1 expressing antibodies with the media optimized for antibody secretion for 3 weeks. After antibody purification, we observed the purified fusion antibodies by SDS-PAGE (Fig. 4B). Obi-ASMase wt showed several degraded forms (arrow bars on Obi-ASMase wt lane in non-reducing, reducing conditions), which might be caused by N-terminal cleavage. Also, Obi-ACDase showed cleaved form (arrow bars on Obi-ACDase lane in reducing condition) in the reducing condition because of the disulfide bonds which stabilize and link two domains (α-domain, β-domain) of ACDase[44]. However, since it did not show a degraded form under non-reducing conditions, Obi-ACDase was thought to maintain an intact form. Fusion Antibodies binding affinity was measured in comparison to

OBI. Ramos cells were incubated with antibodies (7 nM, 21 nM, 70 nM) at 4℃ for 1 hour. There is no difference in the binding affinity of these antibodies, indicating that the binding affinity of the fusion antibodies was almost normal. (Fig. 4C). To identify that these fusion antibodies have ASMase activity, we checked whether they have enzymatic ASMase activity using a fluorogenic substrate of ASMase, HMU-PC. Accuracy of ASMase activity was confirmed by competitive inhibiting activity of SM, a non-fluorogenic substrate of ASMase. In Figure 4 D, compared to OBI, bi-functional fusion antibodies showed noticeable fluorescence and Obi-DEVD-ASMase showed the highest activity among them. These data indicate that we successfully produced and purified the intact fusion antibodies carrying the equivalent affinity and enzymatic activity.

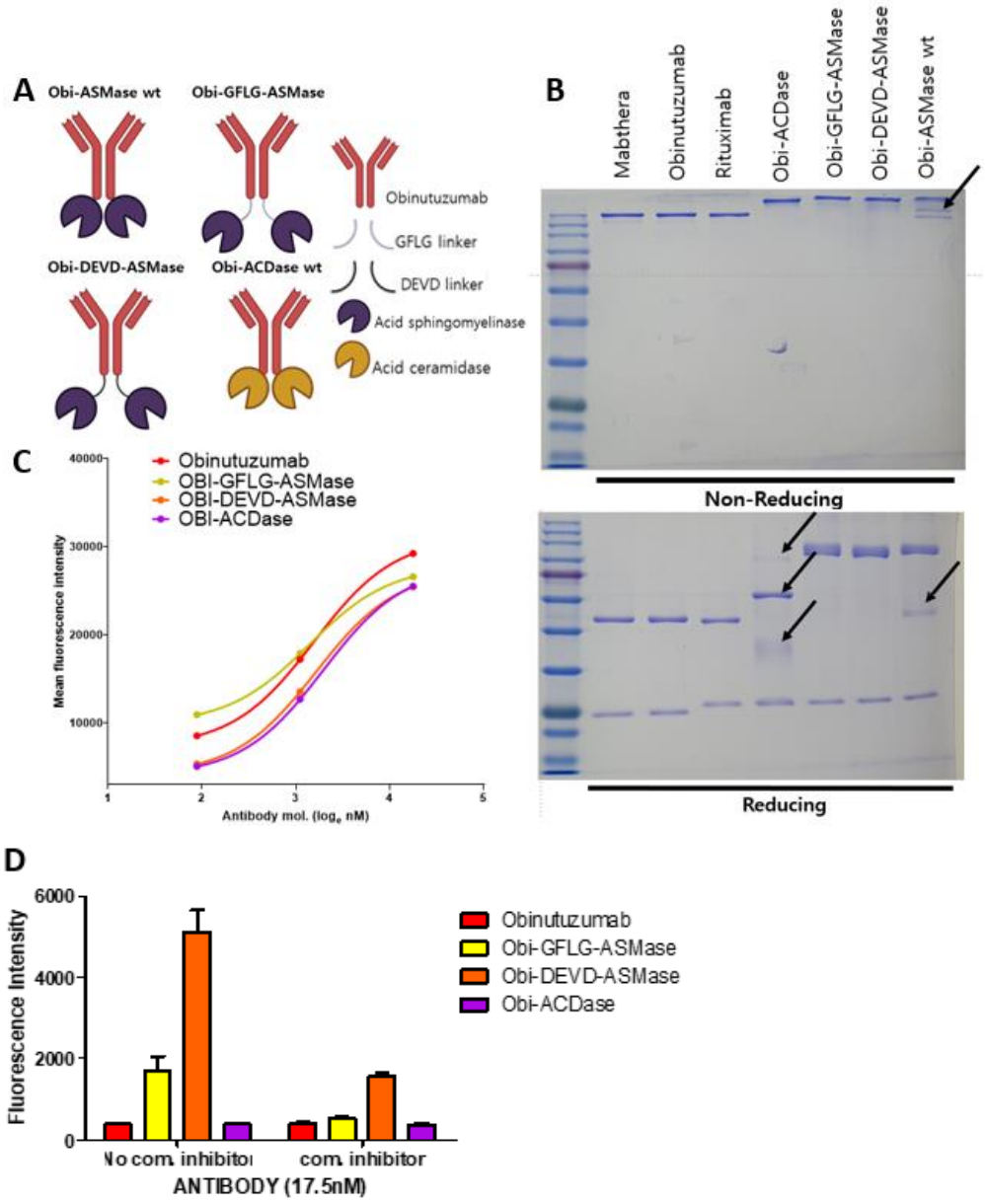

Fig.4 Expression and evaluation of designed Fusion antibodies (A) Schematic image of fusion antibodies. The C-terminal of the OBI heavy chain was fused with the N-terminal of ASMase (purple) or ACDase (yellow). In the case of ASMase, there

are additional two fusion antibodies with –GFLG- or –DEVD- linker. (B) SDS PAGE of antibodies. 7 μM of each antibody was loaded, and each protein was stained with coomassie blue. (C) Binding assay of OBI and fusion antibodies at 7 nM, 21 nM, and 70 nM concentrations. The binding response was conducted at 4℃ for 1hour. The 2nd antibody for primary antibodies, anti-human IgG (Heavy chain + Light chain) Alexa 647, was incubated with Ramos cells at 4℃ for 30 min. The fluorescence was detected by FACSvers. (D) The activity of the enzyme which is fused with antibody. The 17.5 nM antibodies were incubated with 1.32 mmol/L HMU-PC at 37 ℃ for 5 hours. The competitive inhibitor is 10 mM sphingomyelin. In case of no com. Inhibitor, distilled water was added instead.

5. Enhanced DCD and ADCC by ASMase fusion obinutuzumab

Next, we evaluated DCD, ADCC and CDC efficacy of bi-functional fusion antibody whether the fusion antibodies show enhanced B cell depletion ability. Although there was almost no difference in DCD at 7 nM and 21 nM, Obi-GFLG-ASMase and Obi-DEVD-ASMase showed enhanced DCD than OBI at 0.7 nM and 2.1 nM concentrations (Fig, 5A). It appeared that the DCD induced by the fusion antibody reached its maximum faster than the DCD caused by OBI. But, in the case of Obi-ACDase, we observed lower DCD than OBI at every concentration of the antibody. Even when Obi-ACDase-induced DCD was saturated, it was lower than OBI. Compared to OBI, bi-functional fusion antibodies show enhanced ADCC rate at 2.1 nM concentration, but there was no difference at 7 nM, 21 nM (Fig. 5B). Except for Obi-ACDase, this pattern was similar to DCD. A slightly different point is that Obi-DEVD–ASMase killed more target cells than Obi-GFLG-ASMase at 2.1 nM concentration. But CDC of fusion antibodies showed no difference or lower CDC with OBI at every antibody concentration (Fig. 5C). The reason that the CDC of the fusion antibody was similar to or lower than OBI was thought to be because the combined enzyme interferes with the interaction with complement components. Based on this data, the properties of the type II anti-CD20 antibody become stronger, but the properties of the type I anti-CD20 antibody such as CDC remain the same or weaken.

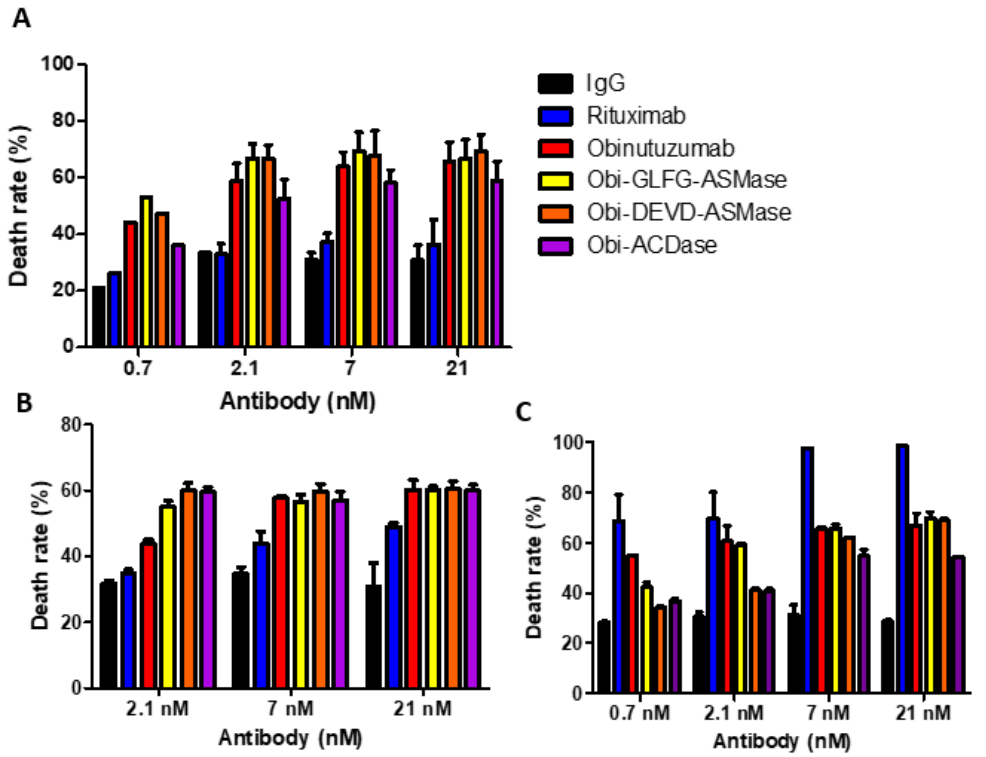

Figure 5. Enhanced B cell depletion by bi-functional fusion antibody. (A) Direct cell death assay according to 0.7 nM 2.1 nM, 7 nM and 21 nM concentrations of RTX, OBI and fusion antibodies. Ramos cells were incubated with antibodies at 37℃ in 5% CO2 for 6 hours. Death rate (%) (100% - % of calcein stained cells) was calculated via FACSverse. (B) Antibody-dependent cellular cytotoxicity of fusion antibodies. Cells were incubated with PBMC in 1:5 ratio and indicated concentration (2.1 nM, 7nM, 21 nM) of antibodies at 37℃ in 5% CO_2 for 4 hours. (C) Complement-dependent cytotoxicity of fusion antibodies. Cells were firstly incubated with antibodies for 10 min, and then incubated with 6 μl of complement at 37℃ in 5% CO_2 for 2 hours. Death rate (%) (100% - % of calcein stained cells) was calculated via FACSverse.

IV. DISCUSSION

Type II anti-CD20 antibodies, including obinutuzumab, exhibit potent DCD and ADCC but relatively weak CDC[11]. It is very interesting that an antibody induces cell death just by attaching it to an antigen, but the exact mechanism has not yet been elucidated. In this study, we elucidated on obinutuzumab-induced DCD by focusing on the mechanism of LMP.

It is known that RTX is internalized by the FcγIIb receptor on the tumor surface[35], but in the case of obinutuzumab, it is not even clear whether it can be internalized. As shown in Figure 1C, we observed that the obinutuzumab is internalized into the acidic compartment by detecting fluorescence of antibodies with a pH-dependent fluorescence. In addition, internalization was compared with filipin and dynasore, the fluorescence change was dramatically decreased (Fig. 2A). To investigate whether this internalization is related to the DCD caused by obinutuzumab, it was confirmed that DCD was reduced by culturing cells with filipin, but not dynasore (Figure 2B).

TRPML channels are Ca^{2+} channels that are associated with lysosome fusion and fission to the various vesicles. Lysosomal lipid storage disorder leads to blocking of TRPML channel activity[41]. In previous research, we observed that OBI suppressed the activity of the TRPML2 channel. Also, the suppressed activity disappeared when filipin was treated, but did not disappear when dynasore was treated. Moreover, as shown in Figure 3, it seems that SM in the plasma membrane moves to the lysosomal membrane and blocks the TRPML2 channel. Taken together, obinutuzumab seems to have two paths for internalization, but the pathway that affects the DCD is caveolae-mediated endocytosis which is accompanied by SM rather than clathrin-mediated endocytosis. Through these findings, we suggest that the lysosomal ASMase catalyzes the internalized SM into ceramide which is subsequently broken into sphingosine by lysosomal ACDase[22,35], then the sphingosine would eventually induce

LMP[22,25].

Through these findings, we suggested that lysosomal ASMase catalyzes internalized SM into ceramide which is subsequently broken into sphingosine by lysosomal ACDase[22,35]. In this suggestion, the sphingosine would eventually induce LMP[22,25].

OBI-induced DCD depends on LMP[14]. When LMP occurs, cell death is induced by the generation of ROS[12,14]. So, we decided to create some constructs for inducing potent and fast LMP compared to OBI by enhanced SMase activity in lysosomes. In Figure 4, we created bi-functional fusion antibodies by fusion of ASMase or ACDase to the C-terminal part of the OBI heavy chain. In the case of Obi-ASMase wt (amino acid residues 47-631), it showed several degraded forms. Perhaps, it is due to N-terminal cleavage which is related to ASMase maturation [42]. The deletion of N-terminal ASMase amino acid residues 47-84 and C-terminus cysteine 631 is required for ASMase's activity[33-34,42-43]. With this in mind, we made fusion antibodies with a modified ASMase (amino acid residues 85-630) and lysosomal degradable linker for membrane docking of ASMase by N-terminal saposin domain [33,42]. As shown in Figure 5A, at low concentrations, the death rate (%) becomes saturated faster than OBI. It is thought that enhanced DCD at low concentrations is probably because N-terminus-exposed ASMase (amino acid residues 85-630) due to cleavage of the linker degrades SM better. But, Although Obi-DEVD-ASMase showed the strongest enzymatic activity than other constructs (Fig. 4D), -GFLG- and –DEVD- linked constructs showed almost no difference in DCD. And, fusion antibody showed no difference in DCD compared to OBI at 7 nM, 21 nM. It is thought that because the internalized SM is limited, the amount of sphingosine accumulated during DCD would be similar in both cases of fusion antibodies. But, Obi-ACDase exhibited lower DCD than OBI. It is thought that this is because the sphingolipid degradation enzyme involved after SM disruption does not affect DCD. Also, this tendency was seen in ADCC as shown in Figure 5B. On the other hand, Obi-ACDase showed higher ADCC

than OBI. Although DCD was lower than OBI, the high ADCC of Obi-ACDase seems to have a different reason from the high ADCC shown in other fusion antibodies. Type I anti-CD20 antibodies such as RTX shows strong CDC after CD20 binding. These antibodies induce rearrangement of CD20 in lipid rafts, which favors complement activation[45]. However, type II anti-CD20 antibodies such as OBI do not form lipid rafts and thus show low CDC. In Figure 5C, Fusion antibodies showed weaker CDC than OBI. This is probably because the changed Fc region blocks the cascade process of complement components or the process of forming a membrane attack complex to induce cell lysis[45]. Based on these results, we suggest that enhanced DCD leads to strong ADCC because it further stimulates the surrounding immune cells.

As a combination treatment strategy with immunomodulatory therapy or bi-specific antibody is becoming the next-generation strategy for the treatment of various lymphoma, ADCC enhancing platform is more demanded for bio-better of target-oriented antibody. This study suggests a strategy for next-generation bio-better of target-oriented antibodies by elucidating the molecular mechanism of DCD induced by OBI as well as evidence that enhanced DCD leads to ADCC improvement.

V. CONCLUSION

In this study, we found that binding of OBI induces endocytosis via caveolae-mediated pathway and blocking of this pathway causes reduced DCD by OBI. Inhibition of endocytosis and depletion of SM in plasma membrane not only reversed TRPML2 Ca^{2+} channel inhibition by OBI, but also decreased DCD by OBI. Enhanced DCD and ADCC by low concentrations of ASMase-fusion OBI demonstrated that degradation of SM in lysosome is a process of DCD. Accordingly, lysosomal sphingolipid metabolism of SM delivered OBI endocytosis mediates DCD by OBI.

REFERENCES

1. Singh R, Shaik S, Negi BS, Rajguru JP, Patil PB,Parihar AS, et al., Non-Hodgkin's lymphoma: A review. Journal of family medicine and primary care, 2020. 9(4): p. 1834-1840.

2. Wang L, Qin W, Huo Y, Li X, Shi Q, Rasko J, Janin A, et al., Advances in targeted therapy for malignant lymphoma. Signal Transduction and Targeted Therapy, 2020. 5(1): p. 15.

3. Raufi A, Ebrahim AS, Al-Katib, Targeting CD19 in B-cell lymphoma: emerging role of SAR3419. Cancer management and research, 2013. 5: p. 225-233.

4. Pavlasova G, Mraz M, The regulation and function of CD20: an "enigma" of B-cell biology and targeted therapy. Haematologica, 2020. 105(6): p. 1494-1506.

5. Casan JML, Wong J, Northcott MJ, Opat S, et al., Anti-CD20 monoclonal antibodies: reviewing a revolution. Human vaccines & immunotherapeutics, 2018. 14(12): p. 2820-2841.

6. Dotan E, Aggarwal C, Smith MR, Impact of Rituximab (Rituxan) on the Treatment of B-Cell Non-Hodgkin's Lymphoma. P & T : a peer-reviewed journal for formulary management, 2010. 35(3): p. 148-157.

7. Lee DSW, Rojas OL, Gommerman JL, B cell depletion therapies in autoimmune disease: advances and mechanistic insights. Nature Reviews Drug Discovery, 2021. 20(3): p. 179-199.

8. Maloney DG, Anti-CD20 Antibody Therapy for B-Cell Lymphomas. New England Journal of Medicine, 2012. 366(21): p. 2008-2016.

9. Beers, SA, Chan CHT, French RR, Cragg MS, Glennie MJ, et al., CD20 as a Target for Therapeutic Type I and II Monoclonal Antibodies. Seminars in Hematology, 2010. 47(2): p. 107-114.

10. Yu Y, Wang M, Zhang X, Li S, Lu Q, Zeng H, et al., Antibody-dependent cellular cytotoxicity response to SARS-CoV-2 in COVID-19 patients. Signal Transduction and Targeted Therapy, 2021. 6(1): p. 346.

11. Tobinai K, Klein C, Oya N, Fingerle-Rowson G, A Review of Obinutuzumab (GA101), a Novel Type II Anti-CD20 Monoclonal Antibody, for the Treatment of Patients with B-Cell Malignancies. Advances in therapy, 2017. **34**(2): p. 324-356.

12. Goede V, Klein C, Stilgenbauer S, Obinutuzumab (GA101) for the Treatment of Chronic Lymphocytic Leukemia and Other B-Cell Non-Hodgkin's Lymphomas: A Glycoengineered Type II CD20 Antibody. Oncology Research and Treatment, 2015. 38(4): p. 185-192.

13. Alduaij W, Ivanov A, Honeychurch J, Cheadle EJ, Potluri S, Lim SH, et al., Novel type II anti-CD20 monoclonal antibody (GA101) evokes homotypic adhesion and actin-dependent, lysosome-mediated cell death in B-cell malignancies. Blood, 2011. 117(17): p. 4519-4529.

14. Honeychurch J, Alduaij W, Azizyan M, Cheadle EJ, Pelicano H, Ivanov A, et al., Antibody-induced nonapoptotic cell death in human lymphoma and leukemia cells is mediated through a novel reactive oxygen species-dependent pathway. Blood, 2012. 119(15): p. 3523-3533.

15. Bonam SR, Wang F, Muller S, Lysosomes as a therapeutic target. Nature Reviews Drug Discovery, 2019. 18(12): p. 923-948.

16. Trivedi PC, Bartlett JJ, Pulinilkunnil T, Lysosomal Biology and Function: Modern View of Cellular Debris Bin. Cells, 2020. 9(5): p. 1131.

17. Aman Y, Schmauck-Medina T, Hansen Ma, Morimoto RI, Simon AK, Bjedov I, et al., Autophagy in healthy aging and disease. Nature Aging, 2021. 1(8): p. 634-650.

18. Glick D, Barth S, Macleod KF, Autophagy: cellular and molecular mechanisms. The Journal of pathology, 2010. 221(1): p. 3-12.

19. Terasawa K, Tomabechi Y, Ikeda M, Ehara H, Kukimoto-Niino M, Wakiyama M, et al., Lysosome-associated membrane proteins-1 and -2 (LAMP-1 and LAMP-2) assemble via distinct modes. Biochemical and Biophysical Research Communications, 2016. 479(3): p. 489-495.

20. Ullio C, Casas J, Brunk UT, Sala G, Fabriàs G, Ghidoni R, et al., Sphingosine mediates TNFα-induced lysosomal membrane permeabilization and ensuing programmed cell death in hepatoma cells. Journal of Lipid Research, 2012. 53(6): p. 1134-1143.

21. Dielschneider RF, Eisenstat H, Mi S, Curtis JM, Xiao W, Johnston JB, et al., Lysosomotropic agents selectively target chronic lymphocytic leukemia cells due to altered sphingolipid metabolism. Leukemia, 2016. 30(6): p. 1290-1300.

22. Wang F, Gómez-Sintes R, Boya P, Lysosomal membrane permeabilization and cell death. Traffic, 2018. 19(12): p. 918-931.

23. Sironi J, Aranda E, Nordstrøm LU, Schwartz EL, Lysosome Membrane Permeabilization and Disruption of the Molecular Target of Rapamycin (mTOR)-Lysosome Interaction Are Associated with the Inhibition of Lung Cancer Cell Proliferation by a Chloroquinoline Analog. Molecular Pharmacology, 2019. 95(1): p. 127-138.

24. Piao S, Amaravadi RK, Targeting the lysosome in cancer. Annals of the New York Academy of Sciences, 2016. 1371(1): p. 45-54.

25. Zhang F, Yang J, Li H, Liu M, Zhang J, Zhao L, et al., Combating rituximab resistance by inducing ceramide/lysosome-involved cell death through initiation of CD20-TNFR1 co-localization. OncoImmunology, 2016. 5(5): p. e1143995.

26. Hammadi M, Youinou P, Tempescul A, Tobón G, Berthou C, Bordron A,, et al., Membrane microdomain sphingolipids are required for anti-CD20-induced death of chronic lymphocytic leukemia B cells. Haematologica, 2012. 97(2): p. 288-296.

27. Tsugawa H, Ikeda K, Tanaka W, Senoo Y, Arita M, Arita M, et al., Comprehensive identification of sphingolipid species by in silico retention

time and tandem mass spectral library. Journal of Cheminformatics, 2017. 9(1): p. 19.

28. Björkbom A, Róg T, Kankaanpää P, Lindroos D, Kaszuba K, Kurita M, N- and O-methylation of sphingomyelin markedly affects its membrane properties and interactions with cholesterol. Biochimica et Biophysica Acta (BBA) - Biomembranes, 2011. 1808(4): p. 1179-1186.

29. Sharpe HJ, Stevens TJ, Munro, A Comprehensive Comparison of Transmembrane Domains Reveals Organelle-Specific Properties. Cell, 2010. 142(1): p. 158-169.

30. Mitsutake S, Zama K, Yokota H, Yoshida T, Tanaka M, Mitsui M, et al., Dynamic modification of sphingomyelin in lipid microdomains controls development of obesity, fatty liver, and type 2 diabetes. The Journal of biological chemistry, 2011. 286(32): p. 28544-28555.

31. Slotte, JP, Biological functions of sphingomyelins. Progress in Lipid Research, 2013. 52(4): p. 424-437.

32. Lewis AC, Wallington-Beddoe CT, Powell JA, Pitson SM, Targeting sphingolipid metabolism as an approach for combination therapies in haematological malignancies. Cell Death Discovery, 2018. 4(1): p. 72.

33. Gorelik A, Illes K, Heinz LX, Superti-Furga G, Nagar B, Crystal structure of mammalian acid sphingomyelinase. Nature communications, 2016. 7: p. 12196-12196.

34. Jenkins RW, Canals D, Hannun YA, Roles and regulation of secretory and lysosomal acid sphingomyelinase. Cellular signalling, 2009. 21(6): p. 836-846.

35. Lim SH, Vaughan AT, Ashton-Key Ma, Williams EL, Dixon SV, Chan HTC, et al., Fc gamma receptor IIb on target B cells promotes rituximab internalization and reduces clinical efficacy. Blood, 2011. 118(9): p. 2530-2540.

36. Sun S, Zu X, Tuo Q, Chen L, Lei X, Li K, et al., Caveolae and caveolin-1 mediate endocytosis and transcytosis of oxidized low density lipoprotein in endothelial cells. Acta Pharmacologica Sinica, 2010. 31(10): p. 1336-1342.

37. Sohn J, Lin Hang, Fritch MR, Tuan RS, Influence of cholesterol/caveolin-1/caveolae homeostasis on membrane properties and substrate adhesion characteristics of adult human mesenchymal stem cells. Stem Cell Research & Therapy, 2018. 9(1): p. 86.

38. Macia E, Ehrlich M, Massol R, Boucrot E, Brunner C, Kirchhausen T, et al., Dynasore, a Cell-Permeable Inhibitor of Dynamin. Developmental Cell, 2006. 10(6): p. 839-850.

39. Cheng X, Shen D, Samie M, Xu H, Mucolipins: Intracellular TRPML1-3 channels. FEBS letters, 2010. 584(10): p. 2013-2021.

40. Cao Q, Yang Y, Zhong XZ, Dong X., The lysosomal Ca(2+) release channel TRPML1 regulates lysosome size by activating calmodulin. The Journal of biological chemistry, 2017. 292(20): p. 8424-8435.

41. Shen D, Wang X, Li X, Zhang X, Yao Z, Dibble S, et al., Lipid storage disorders block lysosomal trafficking by inhibiting a TRP channel and lysosomal calcium release. Nature Communications, 2012. 3(1): p. 731.

42. Lim SM, Yeung K, Trésaugues L, Ling TH, Nordlund P, The structure and catalytic mechanism of human sphingomyelin phosphodiesterase like 3a--an acid sphingomyelinase homologue with a novel nucleotide hydrolase activity. Febs j, 2016. 283(6): p. 1107-23.

43. Jenkins RW, Idkowiak-Baldys J, Simbari F, Canals D, Roddy P, Riner CD, et al., A Novel Mechanism of Lysosomal Acid Sphingomyelinase Maturation: REQUIREMENT FOR CARBOXYL-TERMINAL PROTEOLYTIC PROCESSING*. Journal of Biological Chemistry, 2011. 286(5): p. 3777-3788.

44. Gebai A, Gorelik A, Li Z, Illes K, Nagar B, Structural basis for the activation of acid ceramidase. Nature Communications, 2018. 9(1): p. 1621.

45. Cragg MS, Morgan SM, Chan HT, Morgan BP, Filatov AV, Johnson PW, et al, Complement-mediated lysis by anti-CD20 mAb correlates with segregation into lipid rafts. Blood, 2003. 101(3): p. 1045-52.

ABSTRACT (in Korean)

오비누투주맵의 직접 결합 세포사멸 기전에 있어서 스핑고지질의 역할

<지도교수 김 주 영>

연세대학교 대학원 의과학과

권 선형

오비누투주맵은 항체 의존성 세포 독성이 강화된 CD20 표적 림프종 치료제 3 세대 치료제다. 주목할 점은 오비누투주맵이 항원에 단순히 결합하여 직접 세포 사멸을 유도한다는 것이다. 이 직접 세포 사멸은 LMP 에 의해 세포질로 방출되는 카텝신 B 같은 효소의 세포질로의 방출에 의해 유도되는 것으로 보인다. 그러나 오비누투주맵과 항원의 결합 후 LMP 의 메커니즘은 알려져 있지 않다.

이번 연구에서 우리는 pH 의존적 형광물질을 부착한 오비누투쥬맵을 이용하여 오비누투주맵이 내재화 되어서 리소솜으로 가는 정황을 확인하였다. 또, carveolae 의존적 내재화 억제제로 알려진 filipin 이 오비누투주맵의 결합만으로도 일으키는 직접 세포사멸을 줄이는 것을 보았다. 동시에 라이소좀의 TRPML 칼슘채널의 오비누투쥬맵 처리 이후에 억제되는 현상을 보이고, 세포막을 구성하는 스핑고지질 중 하나인 스핑고마이엘린의 수준과도 관련이 있음을 관찰 했다. 이

현상은 세포막의 스핑고마이엘린을 분해하는 효소에 의해 소실되었고, 또한 이는 오비누투주맵의 직접 결합 세포사멸을 감소시켰다. SM degradation 이 LMP 를 위한 필요과정인지 알아보기 위해서, 리소솜에서 특이적으로 스핑고마이엘린을 분해하는 효소를 오비누투주맵과 융합하여 이중 효과 항체를 만들었다. 이러한 항체는 상대적으로 높은 농도에서는 기존의 오비누투주맵과는 차이를 거의 보이지 않았지만, 낮은 농도에서는 향상된 직접 결합 세포사멸과 항체 의존성 세포 독성을 보임을 관찰했다.

이상의 결과는 오비누투주맵의 결합에 의한 세포사멸은 세포막에 존재하는 스핑고마이엘린이 carveolae 의존적인 세포내유입현상으로 라이소좀에 도달하여 일어나는 현상임을 제안한다. 그리고 유입된 스핑고마이엘린이 연속적으로 분해되는 것이 직접 결합 세포사멸에 필수적인 것으로 생각된다. 또, 낮은 농도의 산성 친화적 스핑고마이엘린 분해효소를 달아준 항체가 보이는 향상된 직접 결합 세포사멸은 이 같은 제안의 뒷받침한다.

핵심 되는 말: 오비누투주맙, CD20, 스핑고마이엘린, 스핑고신, 산성친화적 스핑고마이엘린 분해효소, 산성 친화적 세라마이드 분해효소, LMP